First principles study of the Be–C co-doped MgB_2 system*

Su Xiyu(苏希玉)[1,†], Zhi Xiaofen(支晓芬)[1], Hou Qinying(侯芹英)[2], Cheng Wei(程伟)[1], and Liu Jiaxue(刘佳雪)[1]

(1 Department of Physics & Engineering, Qufu Normal University, Qufu 273165, China)

(2 Library, Qufu Normal University, Qufu 273165, China)

Abstract: We study the Be–C doped MgB_2 system by the first principles method based on density functional theory. The compensation effect between electron type doping and hole type doping is shown in the total density of states on the Fermi level, the real part of optical conductivity, and the number of effective carriers. The compensation mechanisms are discussed. The critical temperatures for different systems are calculated.

Key words: electronic structure; optical properties; MgB_2
DOI: 10.1088/1674-4926/30/11/112001 **PACC:** 7115M; 7000

1. Introduction

Since the discovery of the superconductivity of MgB_2 with critical temperature T_C = 39 K[1], much work has been done to study the underlying superconducting mechanism[2–9]. The isotope effect of boron shows that MgB_2 can be approximately categorized as a BCS-type superconductor[8], and the high T_C originates from the strong electron–phonon couplings. Recently, the impurity effect on MgB_2 has attracted much attention. Actually, both electron type and hole type doping have been already discussed. On electron type doping, Karpinski *et al.* have found that the critical temperature falls and the lattice volume reduces as the Al concentration increases[10]; research on the C-doped MgB_2 system[11] shows similar results. On hole type doping, the unit cell volume and T_C of the Na-doped MgB_2 system increase simultaneously as the Na concentration increases[12]. Experimental research on the Li-doped system shows that the lattice parameter a increases, c changes little, and T_C decreases as the Li concentration increases[13]. It is well known that B layers play an important role in the superconductivity of the MgB_2 system, so if B atoms are substituted by a dopant, the structure, the interband scattering, and the superconductivity of the system can be influenced. The substitution of B by Be is hole type doping, and the substitution of B by C is electron type doping. Both Be doping[14] and C doping[15] have already been studied, but the Be–C co-doped case has not been reported. We study the Be and C co-doped MgB_2 system, i.e. the coexistence of the two kinds of doping. The electronic structure, the optical properties, and the critical temperature of the doped systems are discussed.

2. Computational details

We study C and Be co-doped MgB_2 systems by the first principles method based on density functional theory. All calculations are based on a $2 \times 2 \times 2$ supercell, and a $4 \times 4 \times 3$ k-point mesh in the Brillouin zone is used. The ultra pseudopotential approximation is adopted to describe the interaction between the valence electron and the ion core, and the plane wave set is used to express the electron wave function. The exchange-correlation potential is treated by the generalized gradient approximation, and the precision of the self-consistent energy per atom is 2.0 μeV. The supercell of the Be–C co-doped system is shown in Fig. 1.

3. Results and discussion

3.1. Geometric optimization

Geometric optimization results are listed in Table 1. It is obvious that, compared with the optimized result of the pure system, Be doping makes a, b, c and the unit cell volume bigger; C doping makes a, b, c and the cell volume smaller, while Be–C co-doping makes a and b a little bigger and c bigger, where the change in c is much more obvious than that in a and b, and the cell volumes of the Be–C co-doped system become bigger, too. All these varieties are related to the different intensities of the B–B bond, B–C bond, and B–Be bond. This can also be seen in the bond population of the different systems.

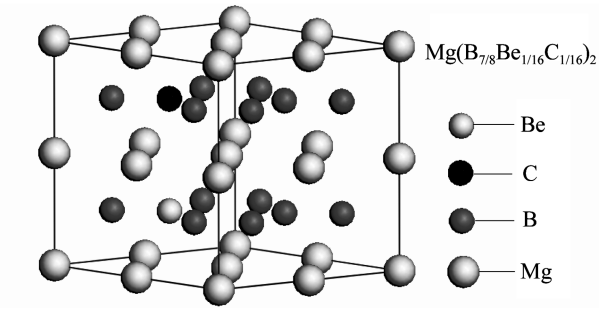

Fig. 1. Supercell of $Mg(B_{7/8}Be_{1/16}C_{1/16})_2$.

* Project supported by the National Natural Science Foundation of China (No. 10775088) and the Key Program of Theoretical Physics of Shandong Province.

† Corresponding author. Email: xiyusu@sina.com

Received 18 April 2009

Table 1. Lattice parameter.

System	Before optimization				After optimization				
	a (10^{-10} m)	b (10^{-10} m)	c (10^{-10} m)	v (10^{-30} m)	a' (10^{-10} m)	b' (10^{-10} m)	c' (10^{-10} m)	v'(supercell) (10^{-30} m)	v'' (unit cell) (10^{-30} m)
MgB_2	6.172	6.172	7.048	232.51	6.093	6.093	7.061	227.17	28.40
$Mg(B_{7/8}Be_{1/8})_2$	6.172	6.172	7.048	232.51	6.202	6.202	7.174	238.50	29.81
$Mg(B_{7/8}C_{1/8})_2$	6.172	6.172	7.048	232.51	6.013	6.013	7.033	220.08	27.51
$Mg(B_{7/8}Be_{1/16}C_{1/16})_2$	6.172	6.172	7.048	232.51	6.099	6.099	7.132	229.28	28.66

Table 2. Bond population of different systems.

System	Bond	Population	Bond length (nm)	Population of unit bond (nm^{-1})	Average population of unit bond of different bond (nm^{-1})
MgB_2	B–B (Covalent bond)	1.43	1.78658	0.80041	0.86624
		1.57	1.74607	0.89916	
$Mg(B_{7/8}Be_{1/8})_2$	B–B (Covalent bond)	1.48	1.78400	0.82960	0.86748
		1.54	1.73263	0.88882	
	B–B (Ionic bond)	−0.26	2.88854	−0.09001	−0.08778
		−0.24	2.88096	−0.08331	
	Be–B	1.35	1.91332	0.70558	0.70995
		1.37	1.90624	0.71869	
$Mg(B_{7/8}C_{1/8})_2$	B–B (Covalent bond)	1.54	1.77359	0.86830	0.89538
		1.61	1.70651	0.94345	
	B–B (Ionic bond)	−0.44	2.98429	−0.14744	−0.14480
		−0.41	2.97512	−0.13969	
	C–B	1.33	1.70217	0.78136	0.79877
		1.40	1.67943	0.83362	
$Mg(B_{7/8}Be_{1/16}C_{1/16})_2$	B–B (Covalent bond)	1.44	1.75280	0.82155	0.87777
		1.61	1.69142	0.95186	
	B–B (Ionic bond)	−0.41	2.95930	−0.13855	−0.13613
		−0.23	2.82294	−0.08147	
	Be–B	1.33	1.89554	0.70165	0.73274
		1.47	1.84922	0.79493	
	C–B	1.31	1.71809	0.76247	0.78695
		1.41	1.68679	0.83591	

The results are given according to the range of population of unit bond.

3.2. Doping and bond population

The bond populations of the different systems are shown in Table 2. In order to study the change of most bonds, the average populations of the unit bond of different bonds are given. The following comparisons are based on the average intensity of the same kind of bond. First, the intensity of the B–B covalent bonds changes a lot, and some B–B ionic bonds exist in each doped system. Compared with the pure system, the B–B covalent bond of the doping systems becomes stronger. The B–B covalent bond of the Be–C co-doped system is stronger than that of the Be doped system, but weaker than that of the C doped system; a similar case happens for the B–B ionic bond. In the Be–C co-doped system, the Be–B bond and C–B bond are weaker than the B–B bond, and the Be–B bond is weaker than the C–B bond. This fact is related to the compensation effect of the two kinds of doping.

3.3. Doping, energy structure and density of states

The calculated band structure and the density of states for different systems are shown in Figs. 2 and 3, respectively. Here, the symmetry k-points are G(0, 0, 0), F(0, 0.5, 0), Q(0, 0.5, 0.5), and Z(0, 0, 0.5). All the systems have metallic

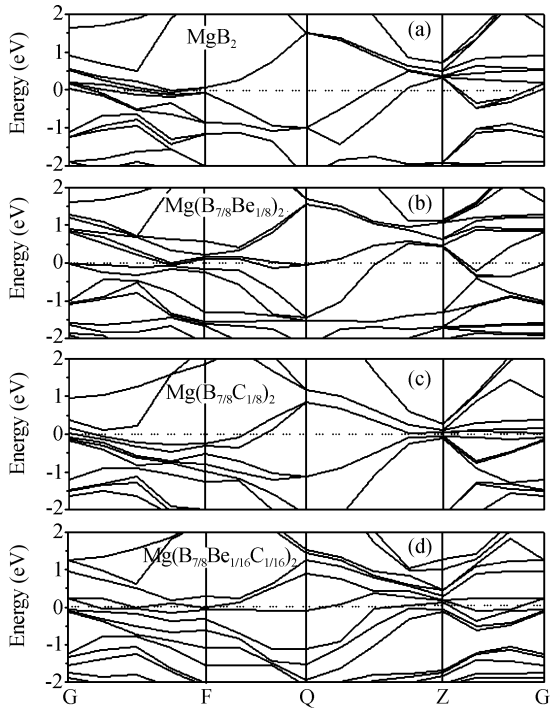

Fig. 2. Energy band of different systems: (a) MgB_2; (b) $Mg(B_{7/8}Be_{1/8})_2$; (c) $Mg(B_{7/8}C_{1/8})_2$; (d) $Mg(B_{7/8}Be_{1/16}C_{1/16})_2$.

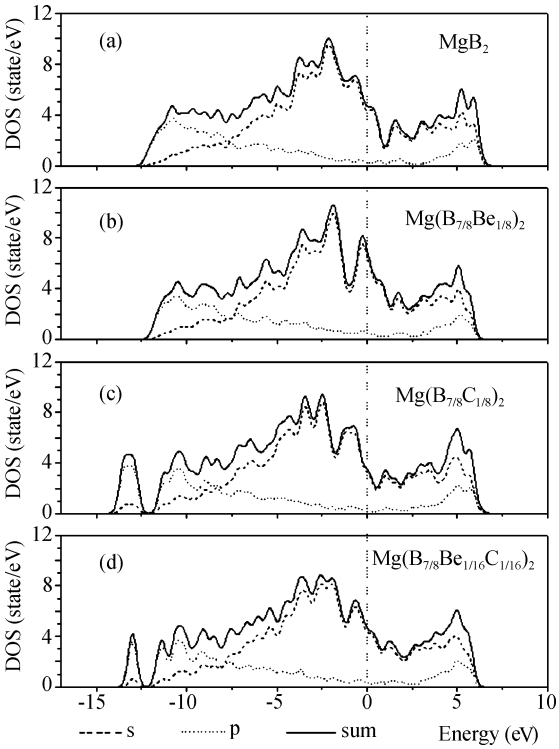

Fig. 3. DOS of different systems: (a) MgB_2; (b) $Mg(B_{7/8}Be_{1/8})_2$; (c) $Mg(B_{7/8}C_{1/8})_2$; (d) $Mg(B_{7/8}Be_{1/16}C_{1/16})_2$.

characteristics, and the evident changes originating from doping are mainly located near the Fermi level. The densities of states on the Fermi level are shown in Table 3. It is known that the states near the Fermi level are primarily contributed by the atoms in the B layer. Additionally, there is a new peak near –13 eV for both C and Be–C doped cases; this is mainly contributed by the C2s states and C2p states. Compared with the pure MgB_2 system, the compensation effect between Be doping and C doping can also be seen as the total DOS on the Fermi level of the Be doped system increases, and that of C doped system decreases; for the Be–C co-doped system, the total DOS on the Fermi level lies between that of the Be doped and C doped systems because of the compensation effect.

Table 3. DOS on the Fermi level of different systems.

System	$N_1(E_F)$ (state/eV)	$N_2(E_F)$ (state/eV)
MgB_2	4.694	3.886
$Mg(B_{7/8}Be_{1/8})_2$	7.135	6.055
$Mg(B_{7/8}C_{1/8})_2$	3.534	3.006
$Mg(B_{7/8}Be_{1/16}C_{1/16})_2$	4.695	3.993

N_1 is the total DOS, and N_2 is the DOS contributed by the atoms in B layer.

Table 4. Critical temperature.

System	T_C (Experiment)	T_C (Theory calculation)
MgB_2	39 K[a)]	38.90 K
$Mg(B_{7/8}Be_{1/8})_2$	33.13 K[b)]	69.8 K
$Mg(B_{7/8}C_{1/8})_2$	18.31 K[c)]	20.76 K
$Mg(B_{7/8}Be_{1/16}C_{1/16})_2$	—	38.93 K

[a)] Ref. [1]; [b)] Ref. [14] ; [c)] Ref. [15].

3.4. Doping and superconductivity

According to BCS theory, the critical temperature T_C of a superconductor is related to DOS on the Fermi level. We can calculate T_C by the McMillan formula.

$$T_C = \frac{\omega}{1.2} \exp \frac{-1.04(1+\lambda)}{\lambda - \mu^*(1+0.62\lambda)}, \tag{1}$$

where $\lambda = [N(E_F)/N_0(E_F)]\,\lambda_0$[16], $\mu^* = [N(E_F)/N_0(E_F)]\,\mu_0^*$, $N_0(E_F)$, λ_0, and μ_0^* are the total DOS on the Fermi level, the effective electron–phonon interaction, and the Coulomb pseudopotential for pure MgB_2, respectively, $N(E_F)$, λ, and μ^* are the corresponding ones for the doped system, and ω is the Debye frequency. In general, we take $\mu_0^* = 0.10$, $\lambda_0 = 0.87$, $\omega = 706$ K. The calculated T_C are shown in Table 4, and are compared with experiments[14, 15]. It should be pointed out that the calculated T_C of the C doped system is in agreement with experiment, while for the Be doped system the agreement is not so good. This means that the superconductivity of the doped MgB_2 cannot be perfectly explained by the BCS theory.

3.5. Doping and optical properties

The compensation effect of Be doping and C doping can also be shown by the optical properties. The interband optical conductivity is determined by the band dispersion and transition matrix element:

$$\sigma_{1,\alpha}(\omega) = \frac{2\pi e^2}{V\omega m^2} \sum_k \sum_{f,i\neq f} |\langle kf|\nabla_\alpha|ki\rangle|^2 f(\varepsilon_{ki}) \times [1 - f(\varepsilon_{kf})]\delta(\varepsilon_{kf} - \varepsilon_{ki} - \hbar\omega), \tag{2}$$

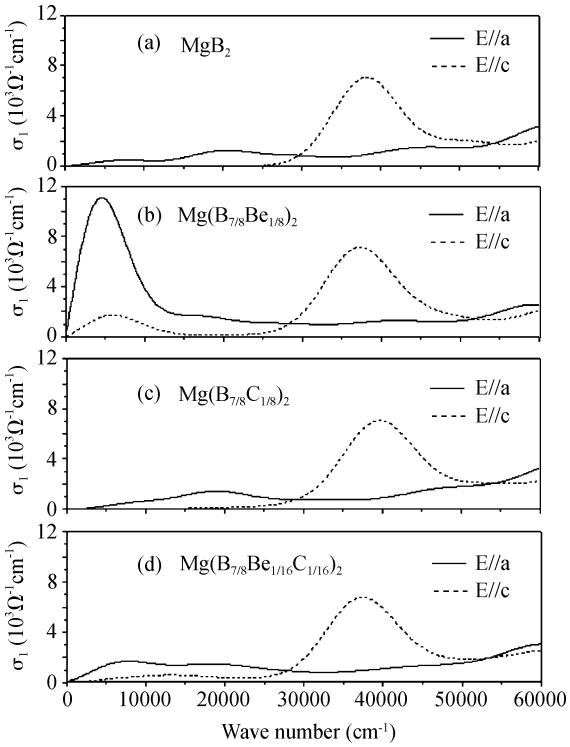

Fig. 4. Optical conductivity of different systems versus wave number.

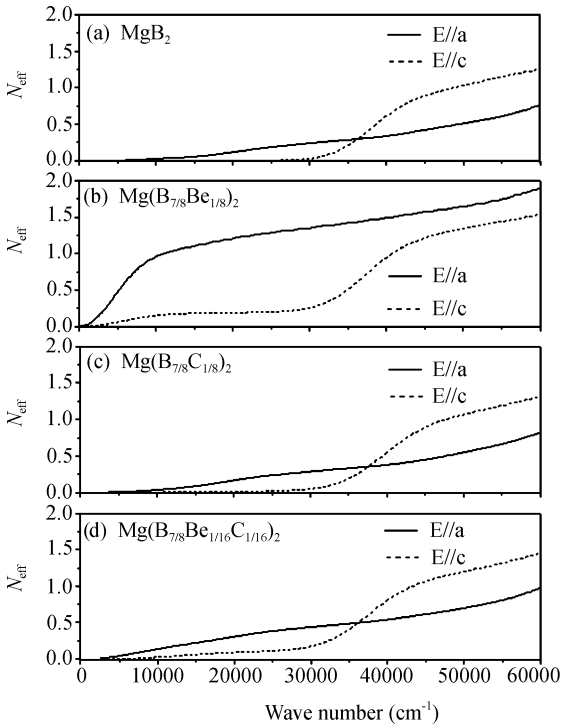

Fig. 5. Effective number of carriers of different systems versus wave number.

where the indices $i(f)$ count bands of initial (final) transition states, V is the unit cell volume, m is the free electron mass, e is the electron charge, and ω is the frequency of normal incident light. The relation between the real part of optical conductivity and the wavenumber is shown in Fig. 4.

There is evident optical anisotropy for each system. When the electric field polarized direction of normal incident light is parallel to the a axis ($E \parallel a$), the optical conductivity is little affected by different doping in the region of–10000 cm^{-1}, and in the region of 0–10000 cm^{-1} the optical conductivity varies sharply. The in-plane optical conductivity shows an intense interband peak at about 5000 cm^{-1} in the Be doping case. In the C doped system, the peak in the region of 0–10000 cm^{-1} becomes smaller; the optical conductivity decreases. The peak mentioned above is reduced in the Be–C co-doped case because of the compensation effect between the two kinds of doping. When $E \parallel c$, the optical conductivity varies mainly in the region of 0–20000 cm^{-1}, there is an interband peak at 6000 cm^{-1}; the conductivity of the C doped system changes little and there is a small peak at 14000 cm^{-1}; this is the result of the compensation effect between the two kinds of doping. The number of effective carriers can be obtained through the optical conductivity as[17]

$$N_{\mathrm{eff}}(\omega) = \frac{2m_0 V_{\mathrm{cell}}}{\pi e^2} \int_0^{\omega} \sigma_1(\omega')\mathrm{d}\omega', \tag{3}$$

where m_0 is the free electron mass, V_{cell} the unit cell volume, e the electron charge, and ω the frequency of normal incident light. The numbers of effective carriers for different systems are shown in Fig. 5. There is evident anisotropy for each system. In the Be doped system, in the region of 0–60000 cm^{-1}, the number of effective carriers for the $E \parallel a$ case is bigger than that for the $E \parallel c$ case. In the Be–C co-doped system, the number of effective carriers for the $E \parallel a$ case is bigger than that for the $E \parallel c$ case in the region of 0–36000 cm^{-1}, while in the region of 36000–60000 cm^{-1}, the number of effective carriers for the $E \parallel a$ case is smaller than that for the $E \parallel c$ case. For the pure system, the C doped system, and the Be–C co-doped system, the relative relations of the number of effective carriers in the $E \parallel a$ case to that of the $E \parallel c$ case are similar. In the case of $E \parallel a$, $N_{\mathrm{eff}}(\omega)$ increases sharply for the Be doped system; for the C doped system, $N_{\mathrm{eff}}(\omega)$ changes little; for the Be–C co-doped system, $N_{\mathrm{eff}}(\omega)$ is smaller than that of the Be doped system, but larger than that of the C doped system because of the compensation effect. In the case of $E \parallel c$, the $N_{\mathrm{eff}}(\omega)$ for different systems are similar to those for the $E \parallel a$ case.

4. Conclusion

We have studied pure MgB_2 and its doped systems by different atoms by the first principles method based on density functional theory. For all the doped systems, the B–B bonds are stronger than those of the pure system. The Be–B bond and C–B bond are weaker than the B–B bond in the $Mg(B_{7/8}Be_{1/16}C_{1/16})_2$ system; there are B–B ionic bonds in the $Mg(B_{7/8}Be_{1/16}C_{1/16})_2$ system. The total density of states on the Fermi level of the $Mg(B_{7/8}Be_{1/16}C_{1/16})_2$ system is higher than that of the C doped system, but lower than that of the Be doped system. The superconductivity critical temperature of the Be–C doped system is higher than that of the C doped system, and lower than that of the Be doped system. When the normal incident direction and the wavenumber of the light is identical, the real part of the optical conductivity

of the Be–C doped system is bigger than that of the C doped system, and smaller than that of the Be doped system in the region of 0–10000 cm^{-1}; while in the region of 0–60000 cm^{-1}, the number of effective carriers of the Be–C doped system is bigger than that of the C doped system, and smaller than that of the Be doped system. This may be accounted for by the compensation effect between the two kinds of doping. Mechanisms for the changes have been discussed.

References

[1] Nagamatsu J, Nakagawa N, Muranaka T, et al. Superconductivity at 39 K in magnesium diboride. Nature (London), 2001, 410(3): 63

[2] Liu Xinyu, Huang Yong, Zeng Zhongming. The progress of superconductivity research of MgB_2. J Mater Sci Eng, 2003, 21(1): 104

[3] Chai Yongquan, Jin Changqing, Liu Banggui. Comparative study on electronic structures of MgB_2-like borides. Acta Physica Sinica, 2003, 52(11): 2883

[4] Tan Mingqiu, Tao Xiangming. Study on the electronic structure of high T_C superconductor MgB_2. Acta Physica Sinica, 2001, 50(6): 1193

[5] Kortus J, Mazin I I, Belashchenk K D, et al. Superconductivity of metallic boron in MgB_2. Phys Rev Lett, 2001, 86: 4656

[6] Liu A Y, Mazin I I, Kortus J. Beyond Eliashberg superconductivity in MgB_2: anharmonicity, two-phonon scattering, and multiple gaps. Phys Rev Lett, 2001, 87: 087005

[7] An J M, Pickett W E. Superconductivity of MgB_2: covalent bonds driven metallic. Phys Rev Lett, 2001, 86: 4366

[8] Bud'ko S L, Lapertot G, Petrovic C, et al. Boron isotope effect in superconducting MgB_2. Phys Rev Lett, 2001, 86: 1877

[9] Kong Y, Dolgov O V, Jensen O, et al. Electron–phonon interaction in the normal and superconducting states of MgB_2. Anderson Phys Rev B, 2001, 64: 020501

[10] Karpinski J, Zhigadlo N D, Schuck G, et al. Al substitution in MgB_2 crystals: influence on superconducting and structural properties. Phys Rev B, 2005, 71: 174506

[11] Szabó P, Samuely P, Holánova Z, et al. Point-contact spectroscopy of Al- and C-doped MgB_2 superconducting energy gaps and scattering studies. Phys Rev B, 2007, 75: 144507

[12] Neaton J B, Perali A. On the possibility of superconductivity at higher temperatures in sp-valent diborides. Condensed Matter, 2001: 0104098

[13] Xiong Yuhua, Li Peijie, Zhang Xiaoping, et al. Influence of doping effect on structure and superconducting properties of MgB_2. Trans Nonferrous Met Soc China, 2003, 13: 1003

[14] Ahn J S, Kim Y J, M S, et al. Structural and superconducting properties of $MgB_{2-x}Be_x$. Phys Rev B, 2002, 65: 172503

[15] Gonnelli R S, Daghero D, Ummarino G A, et al. A point-contact study of the superconducting gaps in Al-substitutedand C-substituted MgB_2 single crystals. J Phys Chem Solids, 2006, 67: 360

[16] Kotegawa H, Ishida K, Kitaoka Y, et al. Evidence for high-frequency phonon mediated S-wave superconductivity: ^{11}B NMR study of Al-doped MgB_2. Phys Rev B, 2002, 66: 064516

[17] Yang H D, Liu H L, Lin J Y, et al. X-ray absorption and optical spectroscopy studies of $(Mg_{1-x}Al_x)B_2$. Phys Rev B, 2003, 68: 092505